OFFICIAL
MASTER COPY

OAK RIDGE NATIONAL LABORATORY
operated by
UNION CARBIDE CORPORATION
NUCLEAR DIVISION
for the
U.S. ATOMIC ENERGY COMMISSION

ORNL-TM-1472

COPY NO. - 60

DATE - October 24, 1966

A MATHEMATICAL MODEL FOR THE HIGH FLUX ISOTOPE REACTOR REACTIVITY CALCULATION

B.R. Lawrence

H.P. Danforth J.B. Bullock

ABSTRACT

A description is given of a model for calculating expected reactivity changes of the High Flux Isotope Reactor by means of an on-line digital computer. The information provided by the model, together with other information, will be used by the on line computer to grant permission for withdrawal of the reactor shim plates. The model uses effective one-energy group microscopic cross sections obtained from the results of separate, more detailed multigroup space-dependent calculations. Perturbation theory with neutron importance weighting is used to account for marked spatial flux distribution changes during the life of a core. The model was programmed for the CDC-1604 computer, and the calculated reactivity change for operation at full power (using preliminary constants) showed an agreement of 0.5% compared with the multigroup space-dependent results.

NOTICE This document contains information of a preliminary nature and was prepared primarily for internal use at the Oak Ridge National Laboratory. It is subject to revision or correction and therefore does not represent a final report.

LEGAL NOTICE

This report was prepared as an account of Government sponsored work. Neither the United States, nor the Commission, nor any person acting on behalf of the Commission:

A. Makes any warranty or representation, expressed or implied, with respect to the accuracy, completeness, or usefulness of the information contained in this report, or that the use of any information, apparatus, method, or process disclosed in this report may not infringe privately owned rights; or

B. Assumes any liabilities with respect to the use of, or for damages resulting from the use of any information, apparatus, method, or process disclosed in this report.

As used in the above, "person acting on behalf of the Commission" includes any employee or contractor of the Commission, or employee of such contractor, to the extent that such employee or contractor of the Commission, or employee of such contractor prepares, disseminates, or provides access to, any information pursuant to his employment or contract with the Commission, or his employment with such contractor.

CONTENTS

Page

Abstract 1

Introduction 4

Model 4

Parameter Values 17

Further Work 20

Notation 22

Appendix I, Fortran Program SC 25

INTRODUCTION

The mathematical model described herein is a requirement in the development of an on-line digital computer system for the High Flux Isotope Reactor (HFIR)[1,2]. The information provided by this model, along with shim plate position and worth, will enable the computer to prevent unsafe automatic shim plate withdrawal due to abnormal core reactivity losses. This task will be accomplished by issuing a shim withdrawal permit to the control system only under normal operating conditions, and will relieve the reactor operator of the present responsibility for the difficult task of assessing reactivity changes from unknown sources.

The model will be the basis for an on-line digital computer program to calculate the expected reactivity balance at all times during the life of a core. The computer will keep an account of changes in reactivity associated with fuel burnup and burnable poison depletion and of the concentration of ^{135}Xe and ^{149}Sm and other fission products, and their effect on reactivity. Changes in reactivity due to temperature changes and other minor effects, such as those due to poisoning of the beryllium reflector and burnup of target materials, are also included.

MODEL

In developing a model to calculate changes in reactivity on an on-line digital computer, typically of only small storage capacity, consideration must be given to simplicity. At the same time, the model must include the essential physical phenomena. In the case of the HFIR it is considered essential to include the effect on reactivity of marked changes in the spatial neutron flux distribution during the life of a core. Separate multigroup space-dependent burnup calculations at full power of 100 Mw have already been performed for the HFIR. Use may be made of the results of these calculations to obtain correctly averaged microscopic cross sections for a consistent one-energy group model.

The starting point will be the one-energy-group-averaged pseudo-steady state diffusion equation

$$\nabla\cdot D[\underline{x},T(\underline{x})]\nabla\phi - \Sigma_a[\underline{x},T(\underline{x})]\phi + \frac{1}{k}\left[\nu\Sigma_f[\underline{x},T(\underline{x})] + 2\Sigma_{n2n}[\underline{x},T(\underline{x})]\right]\phi = 0. \qquad (1)$$

---

[1] L.C. Oakes, A Reactivity Computer for Use with Nuclear Reactor Control Systems, M.S. thesis, Univ. Tenn., ORNL-3685 (Sept. 1964).

[2] F.T. Binford and E.N. Cramer, eds., The High-Flux Isotope Reactor: A Functional Description, ORNL-3572 (1964).

In writing Eq. 1 it is implied that D, Σ_a, $\nu\Sigma_f$, and Σ_{n2n} are constants averaged over the entire neutron energy spectrum from thermal to fission energies at different points in the reactor and are functions of position. The symbol $T(\underline{x})$ represents the temperature at position $(\underline{x})$ in the reactor. The group-averaged constants are temperature dependent because the neutron energy spectrum is dependent on temperature. Σ_a and $\nu\Sigma_f$ can be written as

$$\Sigma_a[\underline{x},T(\underline{x})] = \Sigma_i \sigma_{a_i} [\underline{x},T(\underline{x})]N_i(\underline{x}) ,$$

and

$$\nu\Sigma_f[\underline{x},T(\underline{x})] = \Sigma_j \nu\sigma_{f_j}[\underline{x}, T(\underline{x})]N_j(\underline{x}) .$$

The macroscopic absorption cross section is the sum

$$\Sigma_a = \Sigma_f + \Sigma_c ,$$

where the total macroscopic capture cross section Σ_c includes Σ_{n2n} and $\Sigma_{n\alpha}$ as well as other capture cross sections.

We are interested in changes in reactivity as a result of changes in D, Σ_a, $\nu\Sigma_f$, and Σ_{n2n}. It is convenient to write Eq. 1 in the form

$$J\phi = \frac{1}{k}K\phi, \tag{2}$$

where J is the neutron destruction operator defined by

$$J = -\nabla \cdot D[\underline{x},T(\underline{x})]\nabla + \Sigma_a[\underline{x},T(\underline{x})]$$

and K is the neutron production operator defined by

$$K = \nu\Sigma_f[\underline{x},T(\underline{x})] + 2\Sigma_{n2n}[\underline{x},T(\underline{x})].$$

Applying standard first-order perturbation theory[3] to Eq. 2 we obtain

$$-\delta\rho = \delta\left(\frac{1}{k}\right) = -\frac{\delta k}{k^2} = \frac{\int d\underline{x}\, \phi^+(\underline{x})(\delta J - \frac{1}{k}\,\delta K)\phi(\underline{x})}{\int d\underline{x}\, \phi^+(\underline{x})K\phi(\underline{x})} \tag{3}$$

[3] R. V. Meghreblian and D. K. Holmes, Reactor Analysis, McGraw-Hill, 1960.

where ϕ^+ is the adjoint neutron flux distribution. Since Eq. 1 is self-adjoint, $\phi^+ = \phi$, and Eq. 3 becomes

$$-\delta\rho = \delta\left(\frac{1}{k}\right) = \frac{-\delta k}{k^2} = \frac{\int d\underline{x}\ \phi(\underline{x})(\delta J - \frac{1}{k}\delta K)\phi(\underline{x})}{\int d\underline{x}\ \phi(\underline{x})K\phi(\underline{x})} . \tag{4}$$

It is appropriate at this stage to introduce the following assumptions:

1. Changes in diffusion coefficient with burnup may be neglected, so that

$$\delta J = \delta\Sigma_a[\underline{x},T(\underline{x})].$$

2. Changes in Σ_{n2n} for the beryllium reflector may be ignored, so that

$$\delta K = \delta\nu\Sigma_f[\underline{x},T(\underline{x})].$$

This assumption implies nothing about beryllium poisoning, since this occurs as a result of the buildup of the poison ^{6}Li through a separate Be (n,α) reaction.

With these assumptions, Eq. 4 becomes

$$\delta\rho = \frac{\int d\underline{x}\left\{\frac{1}{k}\delta\nu\Sigma_f[\underline{x},T(\underline{x})] - \delta\Sigma_a[\underline{x},T(\underline{x})]\right\}\phi^2(\underline{x})}{\int d\underline{x}\left\{\nu\Sigma_f[\underline{x},T(\underline{x})] + 2\Sigma_{n2n}[\underline{x},T(\underline{x})]\right\}\phi^2(\underline{x})} . \tag{5}$$

Now,

$$\begin{aligned}\int_r \Sigma[\underline{x},T(\underline{x})]\phi^2(\underline{x})d\underline{x} &= \int_r \Sigma_i N_i(\underline{x})\sigma_i[\underline{x},T(\underline{x})]\phi^2(\underline{x})d\underline{x} \\ &= \Sigma_i\int_r N_i(\underline{x})\sigma_i[\underline{x},T(\underline{x})]\phi^2(\underline{x})d\underline{x} \\ &= \Sigma_i\phi^{2(r)}N_i^{(r)}\sigma_i^{(r)}(T_r)V_r \\ &= \Sigma^{(r)}(T_r)\phi^{2(r)}V_r ,\end{aligned}$$

where we have defined a volume-averaged flux in region r

$$\phi^{(r)} = \frac{\int_r \phi(\underline{x})\ d\underline{x}}{V_r}$$

and a volume-averaged nuclide concentration in region r

$$N_i^{(r)} = \frac{\int_r N_i(\underline{x})\, d\underline{x}}{V_r},$$

and where

$$\Sigma^{(r)}(T_r) = \Sigma_i N_i^{(r)} \sigma_i^{(r)}(T_r) .$$

This implies that $\sigma_i^{(r)}(T_r)$ is defined by

$$\sigma_i^{(r)}(T_r) = \frac{\int_r N_i(\underline{x})\, \sigma_i[\underline{x}, T(\underline{x})]\, \phi^2(\underline{x})\, d\underline{x}}{\phi^{2(r)}\, N_i^{(r)}\, V_r}$$

$$= \frac{V_r^2 \int_r N_i(\underline{x})\, \sigma_i[\underline{x}, T(\underline{x})]\, \phi^2(\underline{x})\, d\underline{x}}{[\int_r \phi(\underline{x})\, d\underline{x}]^2 \int_r N_i(\underline{x})\, d\underline{x}} . \qquad (6)$$

That is, $\int_r \Sigma[\underline{x}, T(\underline{x})]\phi^2(\underline{x})d\underline{x}$ in region r is represented as the product of the square of the average neutron flux in region r, the effective cross section $\Sigma^{(r)}(T_r)$, and the volume of the region. T_r is the average temperature in region r.

A change in macroscopic absorption cross section in region r as a result of burnup and temperature change in that region in the small time interval δt is given to first order by

$$\delta\Sigma_a^{(r)}(T_r) = \frac{\partial\Sigma_a^{(r)}}{\partial T_r}\, \delta T_r + \frac{\partial\Sigma_a^{(r)}}{\partial t}\, \delta t .$$

Similarly,

$$\delta\nu\Sigma_f^{(r)}(T_r) = \frac{\partial\nu\Sigma_f^{(r)}}{\partial T_r}\, \delta T_r + \frac{\partial\nu\Sigma_f^{(r)}}{\partial t}\, \delta t .$$

The contribution to the reactivity change in Eq. 5 from changes in region r is thus:

$$\delta\rho_r = \frac{\left[\frac{1}{k}\,\delta\nu\Sigma_f^{(r)}(T_r) - \delta\Sigma_a^{(r)}(T_r)\right]\phi^{2(r)}\,V_r}{\sum_s\left[\nu\Sigma_f^{(s)}(T_s) + 2\Sigma_{n2n}^{(s)}(T_s)\right]\phi^{2(s)}\,V_s}$$

$$= \frac{\left\{\left[\frac{1}{k}\frac{\partial\nu\Sigma_f^{(r)}}{\partial t} - \frac{\partial\Sigma_a^{(r)}}{\partial t}\right]\delta t + \left[\frac{1}{k}\frac{\partial\nu\Sigma_f^{(r)}}{\partial T_r} - \frac{\partial\Sigma_a^{(r)}}{\partial T_r}\right]\delta T_r\right\}\phi^{2(r)}\,V_r}{\sum_s\left[\nu\Sigma_f^{(s)}(T_s) + 2\Sigma_{n2n}^{(s)}(T_s)\right]\phi^{2(s)}\,V_s}\,, \quad (7)$$

where the s-summation in the denominator is over all regions containing fissile material and beryllium. The component

$$\frac{\left[\frac{1}{k}\frac{\partial\nu\Sigma_f^{(r)}}{\partial Tr} - \frac{\partial\Sigma_a^{(r)}}{\partial T_r}\right]\delta T_r\,\phi^{2(r)}\,V_r}{\sum_s\left[\nu\Sigma_f^{(s)}(T_s) + 2\Sigma_{n2n}^{(s)}(T_s)\right]\phi^{2(s)}\,V_s}$$

is the contribution to the change in reactivity of the reactor due to a change in average temperature of region r so that

$$\frac{\left[\frac{1}{k}\frac{\partial\nu\Sigma_f^{(r)}}{\partial T_r} - \frac{\partial\Sigma_a^{(r)}}{\partial T_r}\right]\phi^{2(r)}\,V_r}{\sum_s\left[\nu\Sigma_f^{(s)}(T_s) + 2\Sigma_{n2n}^{(s)}(T_s)\right]\phi^{2(s)}\,V_s}$$

is identified as the temperature coefficient $\alpha^{(r)}(T_r)$ of the reactor for that region. The contribution to the reactivity change from region r given by Eq. 7 can thus be written as

$$\delta\rho_r = \frac{\left[\frac{1}{k}\frac{\partial\nu\Sigma_f^{(r)}}{\partial t} - \frac{\partial\Sigma_a^{(r)}}{\partial t}\right]\phi^{2(r)}\,V_r}{\sum_s\left[\nu\Sigma_f^{(s)}(T_s) + 2\Sigma_{n2n}^{(s)}(T_s)\right]\phi^{2(s)}\,V_s}\,\delta t + \alpha^{(r)}(T_r)\,\delta T_r\,. \quad (8)$$

It is now necessary to focus attention on the calculation of $\partial\nu\Sigma_f^{(r)}/\partial t$, $\partial\Sigma_a^{(r)}/\partial t$ and $\nu\Sigma_f^{(s)}$ at each time step. To do this it is necessary to know the time behavior of those nuclides which contribute appreciably to $\partial\nu\Sigma_f^{(r)}/\partial t$, $\partial\Sigma_a^{(r)}/\partial t$, and $\nu\Sigma_f^{(s)}$. Changes in concentration of oxygen, aluminum, and water will be assumed to have no effect on reactivity. Equations for the time behavior of nuclides considered to be relevant are as follows:

a. ^{235}U

$$\frac{\partial}{\partial t} N_5(\underline{x},t) = -\phi(\underline{x},t)\, N_5(\underline{x},t)\, \sigma_{a_5}[\underline{x},T(\underline{x})]. \tag{9}$$

b. ^{10}B

$$\frac{\partial}{\partial t} N_{10}(\underline{x},t) = -\phi(\underline{x},t)\, N_{10}(\underline{x},t)\, \sigma_{a_{10}}[\underline{x},T(\underline{x})]. \tag{10}$$

c. ^{135}Xe

$$\frac{\partial}{\partial t} N_I(\underline{x},t) = \gamma_I\, \phi(\underline{x},t)\, N_5(\underline{x},t)\, \sigma_{f_5}[\underline{x},T(\underline{x})] - \{\lambda_I + \phi(\underline{x},t)\, \sigma_{a_I}[\underline{x},T(\underline{x})]\} N_I(\underline{x},t)\ . \tag{11}$$

$$\frac{\partial}{\partial t} N_{xe}(\underline{x},t) = \gamma_{xe}\, \phi(\underline{x},t)\, N_5(\underline{x},t)\, \sigma_{f_5}[\underline{x},T(\underline{x})] + \lambda_I N_I(\underline{x},t) - \{\lambda_{xe} + \phi(\underline{x},t)\, \sigma_{a_{xe}}[\underline{x},T(\underline{x})]\}\, N_{xe}(\underline{x},t)\ . \tag{12}$$

d. ^{149}Sm

$$\frac{\partial}{\partial t} N_{pm}(\underline{x},t) = \gamma_{pm}\, \phi(\underline{x},t)\, N_5(\underline{x},t)\, \sigma_{f_5}[\underline{x},T(\underline{x})] - \{\lambda_{pm} + \phi(\underline{x},t)\, \sigma_{a_{pm}}[\underline{x},T(\underline{x})]\} N_{pm}(\underline{x},t)\ . \tag{13}$$

$$\frac{\partial}{\partial t} N_{sm}(\underline{x},t) = \gamma_{sm}\, \phi(\underline{x},t)\, N_5(\underline{x},t)\, \sigma_{f_5}[\underline{x},T(\underline{x})] + \lambda_{pm}\, N_{pm}(\underline{x},t) - \sigma_{a_{sm}}[\underline{x},T(\underline{x})]\, \phi(\underline{x},t)\, N_{sm}(\underline{x},t)\ . \tag{14}$$

e. General fission products other than ^{135}Xe and ^{149}Sm

$$\frac{\partial}{\partial t} \Sigma_{FP}(\underline{x},t) = \alpha_{FP}\, \phi(\underline{x},t)\, N_5(\underline{x},t)\, \sigma_{f_5}[\underline{x},T(\underline{x})]. \tag{15}$$

f. ^{6}Li

$$\frac{\partial}{\partial t} N_{Li}(\underline{x},t) = \sigma_{n\alpha}[\underline{x},T(\underline{x})]\, \phi(\underline{x},t)\, N_{Be}(\underline{x},t) - \sigma_{a_{Li}}[\underline{x},T(\underline{x})]\, \phi(\underline{x},t)\, N_{Li}(\underline{x},t)\ . \tag{16}$$

Equations for changes in concentration of target materials are not included. Since the reactivity change associated with the target is small over the lifetime of a core, this will be taken into account by a simple linear representation, the form of which is obtained from separate reactor physics calculations, superimposed on the other reactivity changes included in the model. By regarding ^{6}Li as the only significant beryllium poison, we are ignoring the buildup of the poison $^{3}He_2$ which is formed from the decay of tritium in beryllium with a half-life of 12.5 years.

Integration of both sides of Eq. 9 over region r and dividing by the volume of region r gives

$$\begin{aligned} \frac{\partial}{\partial t} N_5^{(r)}(t) &= -\frac{1}{V_r} \int_r \phi(\underline{x},t)\, N_5(\underline{x},t)\, \sigma_{a_5}[\underline{x},T(\underline{x})]d\underline{x} \\ &= -\phi^{(r)}(t)\, N_5^{(r)}(t)\, \tilde{\sigma}_{a_5}^{(r)}\ , \end{aligned} \tag{17}$$

which implies that

$$\tilde{\sigma}_{a_5}^{(r)} = \frac{V_r \int_r \phi(\underline{x},t)\, N_5(\underline{x},t)\, \sigma_{a_5}[\underline{x},T(\underline{x})]\, d\underline{x}}{\int_r \phi(\underline{x},t)\, d\underline{x} \int_r N_5(\underline{x},t)\, d\underline{x}}\ . \tag{18}$$

Equation 18 shows that $\tilde{\sigma}_{a_5}^{(r)}$ is actually time dependent, but since this is expected to be slight, it will be assumed that $\tilde{\sigma}_{a_5}^{(r)}$ does not change with time. The right-hand side of Eq. 17 is the product of the average flux in the region, the average nuclide concentration in the region, and the effective microscopic cross section (Eq. 18). Collecting the result of Eq. 17 and doing the same for Eqs. 10 through 16, we arrive at the following equa-

tions for the time behavior of the average concentrations of the relevant nuclides in region r:

$$\frac{\partial}{\partial t} N_5^{(r)}(t) = -\phi^{(r)}(t)\, N_5^{(r)}(t)\, \tilde{\sigma}_{a_5}^{(r)} , \tag{19}$$

$$\frac{\partial}{\partial t} N_{10}^{(r)}(t) = -\phi^{(r)}(t)\, N_{10}^{(r)}(t)\, \tilde{\sigma}_{a_{10}}^{(r)} , \tag{20}$$

$$\frac{\partial}{\partial t} N_I^{(r)}(t) = \gamma_I\, \phi^{(r)}(t)\, N_5^{(r)}(t)\, \tilde{\sigma}_{f_5}^{(r)} - [\lambda_I + \phi^{(r)}(t)\, \tilde{\sigma}_{a_I}^{(r)}]\, N_I^{(r)}(t) , \tag{21}$$

$$\frac{\partial}{\partial t} N_{xe}^{(r)}(t) = \gamma_{xe}\, \phi^{(r)}(t)\, N_5^{(r)}(t)\, \tilde{\sigma}_{f_5}^{(r)} + \lambda_I\, N_I^{(r)}(t) - [\lambda_{xe} + \phi^{(r)}(t)\, \tilde{\sigma}_{a_{xe}}^{(r)}]\, N_{xe}^{(r)}(t) , \tag{22}$$

$$\frac{\partial}{\partial t} N_{pm}^{(r)}(t) = \gamma_{pm}\, \phi^{(r)}(t)\, N_5^{(r)}(t)\, \tilde{\sigma}_{f_5}^{(r)} - [\lambda_{pm} + \phi^{(r)}(t)\, \tilde{\sigma}_{a_{pm}}^{(r)}]\, N_{pm}^{(r)}(t) , \tag{23}$$

$$\frac{\partial}{\partial t} N_{sm}^{(r)}(t) = \gamma_{sm}\, \phi^{(r)}(t)\, N_5^{(r)}(t)\, \tilde{\sigma}_{f_5}^{(r)} + \lambda_{pm}\, N_{pm}^{(r)}(t) - \tilde{\sigma}_{a_{sm}}^{(r)}\, \phi^{(r)}(t)\, N_{sm}^{(r)}(t) , \tag{24}$$

$$\frac{\partial}{\partial t} \Sigma_{FP}^{(r)}(t) = \alpha_{FP}\, \phi^{(r)}(t)\, N_5^{(r)}(t)\, \tilde{\sigma}_{f_5}^{(r)} , \tag{25}$$

$$\frac{\partial}{\partial t} N_{Li}^{(r)}(t) = \tilde{\sigma}_{n\alpha}^{(r)}\, \phi^{(r)}(t)\, N_{Be}^{(r)}(t) - \tilde{\sigma}_{a_{Li}}^{(r)}\, \phi^{(r)}(t)\, N_{Li}^{(r)}(t) . \tag{26}$$

The effective cross sections appearing in Eqs. 19 through 26 are defined in the manner of Eq. 18 and are assumed to be time independent.

The HFIR spatial regions are shown in Fig. 1. The various essential contributions to $\partial\nu\Sigma_f^{(r)}/\partial t$ and $\partial\Sigma_a^{(r)}/\partial t$ are shown in Table I and Fig. 2. Since the number of beryllium atoms burned in the reflector will be a very small fraction of the total number of beryllium atoms initially present in this region, $N_{Be}^{(7)}$ is regarded as being constant with time. The total reactivity change in time interval δt is the sum of the contributions from all regions and is, from Eq. 8

$$\delta\rho = \sum_r \delta\rho_r = \frac{\sum_r \left[\frac{1}{k}\frac{\partial}{\partial t}\nu\Sigma_f^{(r)} - \frac{\partial}{\partial t}\Sigma_a^{(r)} \right] \phi^{2(r)} V_r}{\sum_s \left[\nu\Sigma_f^{(s)} + 2\Sigma_{n2n}^{(s)} \right] \phi^{2(s)} V_s} \delta t + \sum_r \alpha^{(r)} \delta T_r ,$$

$$\left[\frac{1}{k}\nu\sigma_{f_5}^{(3)} \frac{\partial}{\partial t} N_5^{(3)}(t) - \sigma_{a_5}^{(3)} \frac{\partial}{\partial t} N_5^{(3)}(t) - \sigma_{a_{10}}^{(3)} \frac{\partial}{\partial t} N_{10}^{(3)}(t) \right.$$

$$\left. - \sigma_{a_{xe}}^{(3)} \frac{\partial}{\partial t} N_{xe}^{(3)}(t) - \sigma_{a_{sm}}^{(3)} \frac{\partial}{\partial t} N_{sm}^{(3)}(t) - \frac{\partial}{\partial t}\Sigma_{FP}^{(3)}(t) \right] \phi^{2(3)} V_3$$

$$= \frac{-\sigma_{a_{Li}}^{(7)} \frac{\partial}{\partial t} N_{Li}^{(7)}(t)\, \phi^{2(7)} V_7}{\left[\nu\sigma_{f_5}^{(3)} N_5^{(3)}(t)\, \phi^{2(3)} V_3 + 2\sigma_{n2n}^{(7)} N_{Be}^{(7)} \phi^{2(7)} V_7 \right]} \delta t + \sum_r \alpha^{(r)} \delta T_r \tag{27}$$

The Be(n,2n) reaction and the Be(n,α) reaction both occur in the reflector with fast neutrons (>0.7 Mev) and will be relatively unaffected by the position of the shim plates between the core and reflector. The main influence will be the fast neutron production rate in the core. Furthermore, both of these reaction rates are small compared with the fission neutron release rate. It will suffice to write

$$2\sigma_{n2n}^{(7)} N_{Be}^{(7)} \phi^{(7)} V_7 = R_{n2n} \nu\Sigma_f^{(3)} \phi^{(3)} V_3 , \tag{28}$$

$$\tilde{\sigma}_{n\alpha}^{(7)} N_{Be}^{(7)} \phi^{(7)} V_7 = R_{n\alpha} \nu\Sigma_f^{(3)} \phi^{(3)} V_3 , \tag{29}$$

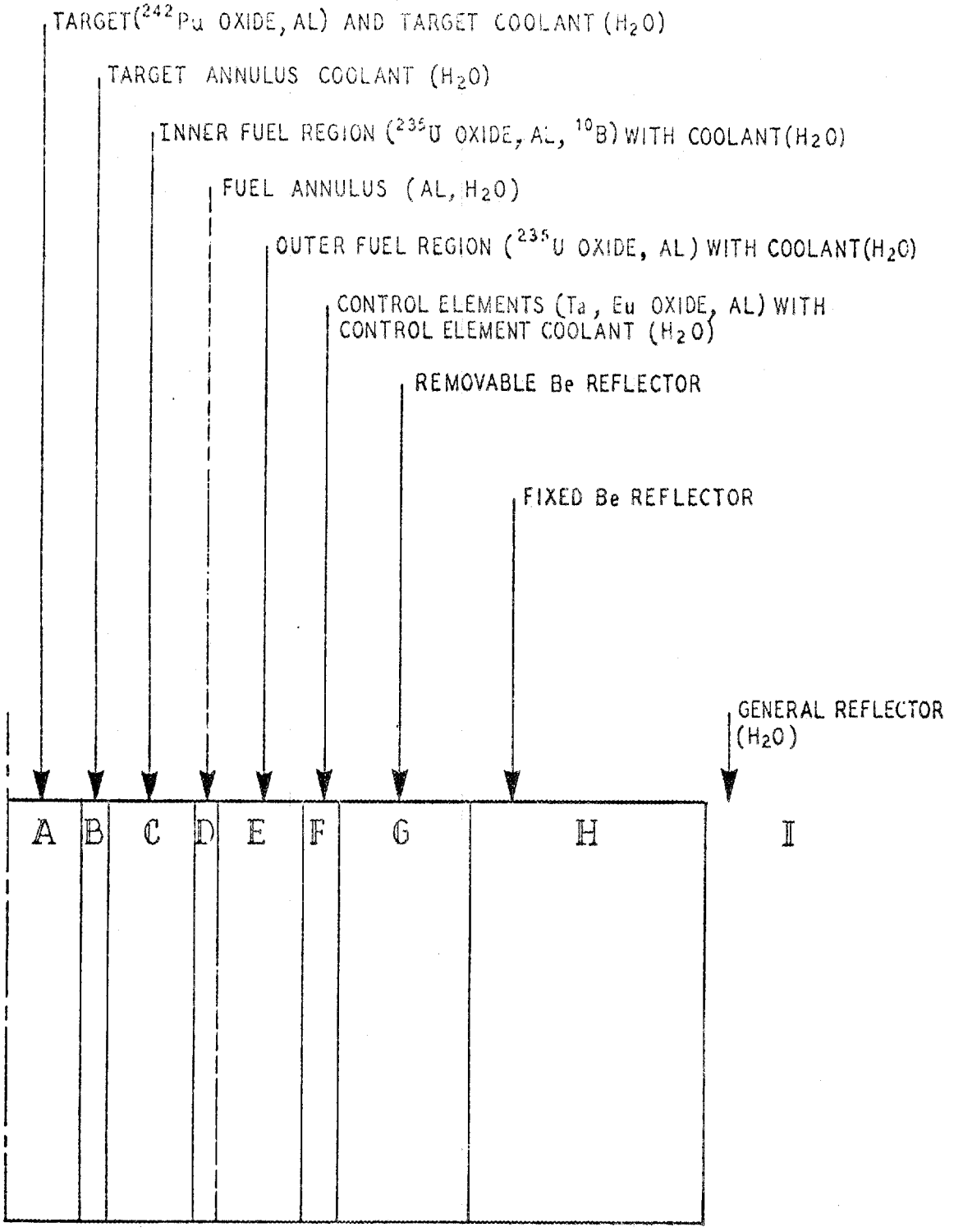

Fig. 1. Diagram of HFIR Spatial Regions (not to scale).

Table I. Contributions to $\frac{\partial}{\partial t}\nu\Sigma_f^{(r)}$ and $\frac{\partial}{\partial t}\Sigma_a^{(r)}$ from HFIR Spatial Regions

Region Index r	Identification in Fig. 1	$\frac{\partial}{\partial t}\nu\Sigma_f^{(r)}$	$\frac{\partial}{\partial t}\Sigma_a^{(r)}$
3(fuel)	C,E	$\nu\sigma_{f_5}^{(3)}\frac{\partial}{\partial t}N_5^{(3)}(t)$	$\sigma_{a_5}^{(3)}\frac{\partial}{\partial t}N_5^{(3)}(t) +$ $\sigma_{a_{10}}^{(3)}\frac{\partial}{\partial t}N_{10}^{(3)}(t) +$ $\sigma_{a_{xe}}^{(3)}\frac{\partial}{\partial t}N_{xe}^{(3)}(t) +$ $\sigma_{a_{sm}}^{(3)}\frac{\partial}{\partial t}N_{sm}^{(3)}(t) +$ $\frac{\partial}{\partial t}\Sigma_{FP}^{(3)}(t)$
4(fuel coolant)	C,E	0	0
7(beryllium)	G,H	0	$\sigma_{a_{Li}}^{(7)}\frac{\partial}{\partial t}N_{Li}^{(7)}(t)$

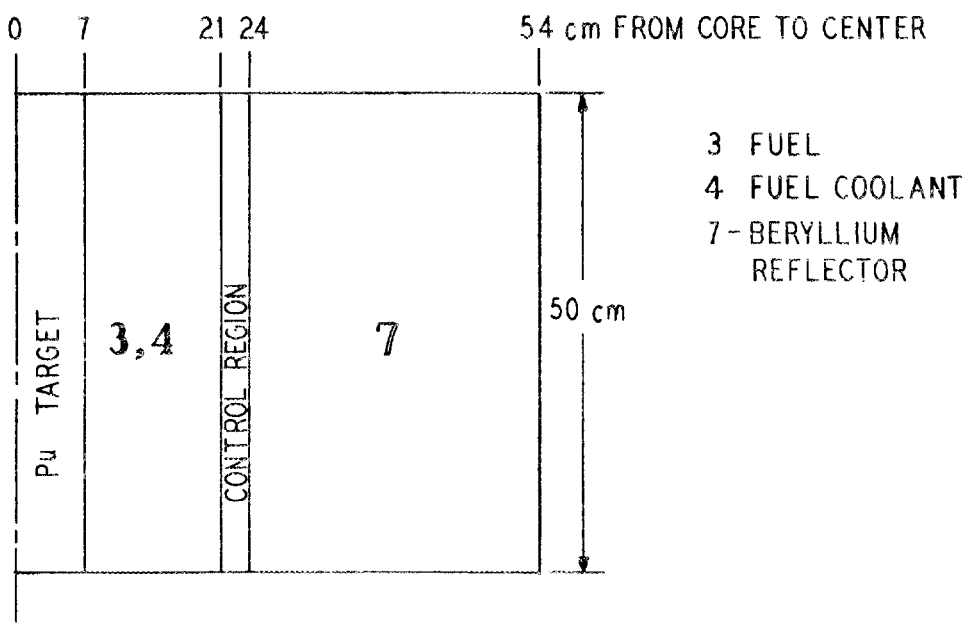

Fig. 2. Diagram of HFIR Spatial Regions Used in Model (dimensions are approximate).

where R_{n2n} and $R_{n\alpha}$ are constants. With this simplification the denominator of Eq. 27 becomes

$$\nu\Sigma_f^{(3)}\,\phi^{2(3)}\,V_3 + 2\sigma_{n2n}^{(7)}\,N_{Be}^{(7)}\,\phi^{2(7)}\,V_7 = \nu\Sigma_f^{(3)}\,\phi^{2(3)}\,V_3 + R_{n2n}\,\nu\Sigma_f^{(3)}\,\phi^{(3)}\,V_3\,\phi^{(7)}$$

$$= \nu\Sigma_f^{(3)}\phi^{(3)}V_3\left[\phi^{(3)} + R_{n2n}\phi^{(7)}\right]. \quad (30)$$

The ratio of the average flux in region r to the average flux in the fuel region (r = 3) will be assumed to be linearly dependent on shim plate position s; that is,

$$\phi^{(r)}(t) = \left[\gamma^{(r)} + \beta^{(r)}s\right]\phi^{(3)}(t)\ . \quad (31)$$

With this representation the denominator of Eq. 27 can be further written

$$\nu\Sigma_f^{(3)}\,\phi^{(3)}\,V_3\left[1 + R_{n2n}(\gamma^{(7)} + \beta^{(7)}s)\right]\phi^{(3)}\ .$$

With a similar simplification, Eq. 26 with r = 7 becomes

$$\frac{\partial}{\partial t}N_{Li}^{(7)}(t) = \frac{R_{n\alpha}\,\nu\Sigma_f^{(3)}\,\phi^{(3)}\,V_3}{V_7} - \tilde{\sigma}_{a_{Li}}^{(7)}\,\phi^{(7)}\,N_{Li}^{(7)}(t)\ . \quad (32)$$

Using Eqs. 19 through 25 and Eqs. 30 and 32, Eq. 27 can be written

$$\delta\rho = \frac{\left\{ \left[\tilde{\sigma}^{(3)}_{a_5}\sigma^{(3)}_{a_5} - \frac{1}{k}\tilde{\sigma}^{(3)}_{a_5}\nu\sigma^{(3)}_{f_5} - \gamma_{xe}\,\tilde{\sigma}^{(3)}_{f_5}\sigma^{(3)}_{a_{xe}} - \gamma_{sm}\,\tilde{\sigma}^{(3)}_{f_5}\sigma^{(3)}_{a_{sm}} - \alpha_{FP}\,\tilde{\sigma}^{(3)}_{f_5} \right] N^{(3)}_5(t)\,\phi^{(3)}(t) + \phi^{(3)}(t)\,\tilde{\sigma}^{(3)}_{a_{10}}\sigma^{(3)}_{a_{10}}N^{(3)}_{10}(t) - \lambda_I\sigma^{(3)}_{a_{xe}}\,N^{(3)}_I(t) + \left[\lambda_{xe}\sigma^{(3)}_{a_{xe}} + \phi^{(3)}(t)\,\tilde{\sigma}^{(3)}_{a_{xe}}\sigma^{(3)}_{a_{xe}}\right] N^{(3)}_{xe}(t) - \lambda_{pm}\sigma^{(3)}_{a_{sm}}N^{(3)}_{pm}(t) + \phi^{(3)}(t)\,\tilde{\sigma}^{(3)}_{a_{sm}}\sigma^{(3)}_{a_{sm}}N^{(3)}_{sm}(t) \right\} \phi^{2(3)}\,V_3 + \phi^{3(7)}V_7\,\tilde{\sigma}^{(7)}_{a_{Li}}\sigma^{(7)}_{a_{Li}}N^{(7)}_{Li}(t) - R_{n\alpha}\nu\sigma^{(3)}_{f_5}N^{(3)}_5(t)\,\phi^{(3)}V_3\,\phi^{2(7)}\sigma^{(7)}_{a_{Li}}}{\nu\sigma^{(3)}_{f_5}\,N^{(3)}_5(t)\,\phi^{2(3)}V_3\left\{1 + R_{n2n}\left[\gamma^{(7)} + \beta^{(7)}s\right]\right\}}\,\delta t + \sum_r \alpha^{(r)}\,\delta T_r\,. \tag{33}$$

In the normal course of operation, k is approximately equal to 1 in Eq. 33. In special situations, such as an ac power failure or an accidental shim-plate drop, the reactor will undergo transients in which k will depart from unity for short intervals of time. Typically, in such transients the contribution to $\delta\rho$ from xenon will be so predominant that no significant error will be introduced by always using k = 1 in Eq. 33.

Only two temperatures need be included in the sum $\sum_r \alpha^{(r)}\delta T_r$, these being the average fuel temperature T_3 and the average fuel coolant temperature T_4. The required temperatures T_3 and T_4 are not available from sensors and will be calculated by the on-line computer. The following equations, which include delayed heating effects, will be used to represent the behavior of T_3 and T_4:

$$P = \Gamma\,\tilde{\sigma}_{f_5}{}^{(3)}N^{(3)}_5(t)\,\phi^{(3)}(t)\,V_3\,, \tag{34}$$

$$\Psi = (1 - \gamma_h)P + w\,, \tag{35}$$

$$\frac{dw}{dt} + \lambda_h w = \lambda_h\gamma_h P\,, \tag{36}$$

$$M_f C_f \frac{dT_3}{dt} = \Gamma_f \Psi - h_{fc} A_f (T_3 - T_4) , \tag{37}$$

$$M_c C_c \frac{dT_4}{dt} = h_{fc} A_f (T_3 - T_4) - \frac{2M_c C_c}{\tau_c}(T_4 - T_{in}) . \tag{38}$$

Since the thermal time constants for the HFIR are small compared with other time constants in the model, the relations

$$\Gamma_f \Psi = h_{fc} A_f (T_3 - T_4) \tag{39}$$

$$h_{fc} A_f (T_3 - T_4) = \frac{2M_c C_c}{\tau_c}(T_4 - T_{in}) \tag{40}$$

together with Eqs. 34 through 36 will be used instead of Eqs. 37 and 38 to calculate T_3 and T_4 from Ψ and T_{in}.

Equations 19 through 25, 32, 33, 34 through 36, 39, and 40 will be used as the basis for a computer program for the on-line computation of the required reactivity changes in the HFIR. It is seen that we essentially require $\phi^{(3)}(t)$, the concentrations of various nuclides at each point in time which are calculated by the on-line computer, s, and T_{in}. The values of $\phi^{(3)}(t)$, s, and T_{in} can be calculated from information provided by the HFIR control system instrumentation.

PARAMETER VALUES

Some preliminary idea of the magnitude of the effective cross sections $\sigma_i^{(r)}$ and $\tilde{\sigma}_i^{(r)}$ can be obtained from cross-section compilations, and improvement of these initial estimates can be achieved by varying these values so as to make the reactivity calculations using the above model agree as closely as possible with the 100-Mw constant power multigroup space-dependent reactor physics calculations that have already been performed for the HFIR. The effective cross-section estimates thus obtained will at least approximately reproduce the reactor physics reactivity lifetime curve at full power when used in the on-line model, and there can be some confidence in using them in the on-line model for calculations involving time-varying power. Such estimates of parameters that relate to burnup have been obtained by least-squares techniques using a general least-squares program[4] and are tabulated in Table II. In setting up Table II a thermal flux is used for convenience as the reference flux,

[4] W. R. Busing and H. A. Levy, ORGLS: A General Least Squares Program, ORNL-TM-271 (August 1962).

Table II. Symbols and Their Numerical Values

Mathematical Symbol	Computer Fortran Symbol	Numerical Value
$\tilde{\sigma}_{a_5}^{(3)}$	SA5S3	4.846×10^{-22}
$\sigma_{a_5}^{(3)}$	SA53	7.200×10^{-22}
$\nu\sigma_{f_5}^{(3)}$	USF53	8.548×10^{-22}
$\tilde{\sigma}_{f_5}^{(3)}$	SF5S3	3.929×10^{-22}
$\tilde{\sigma}_{a_{10}}^{(3)}$	SA10S3	3.650×10^{-21}
$\sigma_{a_{10}}^{(3)}$	SA103	5.435×10^{-21}
$\tilde{\sigma}_{a_I}^{(3)}$	SAIS3	0.0
λ_I	AMDAI	2.87×10^{-5}
γ_I	GI	6.1×10^{-2}
$\tilde{\sigma}_{a_{xe}}^{(3)}$	SAXES3	1.808×10^{-18}
$\sigma_{a_{xe}}^{(3)}$	SAXE3	2.690×10^{-18}
λ_{xe}	AMDAXE	2.09×10^{-5}
γ_{xe}	GXE	1.90×10^{-3}
$\tilde{\sigma}_{a_{pm}}^{(3)}$	SAPMS3	0.0
λ_{pm}	AMDAPM	2.585×10^{-6}
γ_{pm}	GPM	1.646×10^{-2}
$\tilde{\sigma}_{a_{sm}}^{(3)}$	SASMS3	6.339×10^{-20}
$\sigma_{a_{sm}}^{(3)}$	SASM3	8.66×10^{-20}

Table II. (continued)

Mathematical Symbol	Computer Fortran Symbol	Numerical Value
γ_{sm}	GSM	0.0
α_{FP}	ALPFP	1.480×10^{-22}
$\tilde{\sigma}_{a_{Li}}^{(7)}$	SALIS7	9.450×10^{-22}
$\sigma_{a_{Li}}^{(7)}$	SALI7	9.450×10^{-22}
R_{n2n}	RN2N	0.01
$R_{n\alpha}$	RNA	0.01
$\phi^{(3)}(0)$	F3	3.329×10^{4}
$N_5(0)$	B(1)	4.726×10^{20}
$N_{10}(0)$	B(2)	3.303×10^{18}
$V^{(3)}$	V3	5.095×10^{4}
$V^{(7)}$	V7	3.710×10^{5}
$\beta^{(7)}$	BETA7	0.0
$\gamma^{(7)}$	GAM7	0.02

and effective cross sections appearing in the table are such that, when multiplied by the corresponding thermal flux, the correct reaction rate for neutrons of all energies results. A plot (Fig. 3) of reactivity vs time for a single core life gives reactivity changes due to burnup at full-power operation using the values of Table II in the Fortran Program SC (Appendix I) for the above model. Figure 3 also shows similar results obtained from preliminary multigroup space-dependent reactor physics calculations[5] for comparison. Agreement is seen to be of the order of 0.5%.

FURTHER WORK

Further work will be aimed at the inclusion of the temperature effects and the modification of the computer program to make it compatible with the on-line computer system. Operating experience on the HFIR along with data from future experiments will make it possible to fit the model more closely to the actual reactor once the on-line computer system is in operation. Studies will be made to ascertain whether or not the program, in its present state of development, can be applied to all transient conditions.

---

[5] T. M. Sims and R. D. Cheverton, private communication.

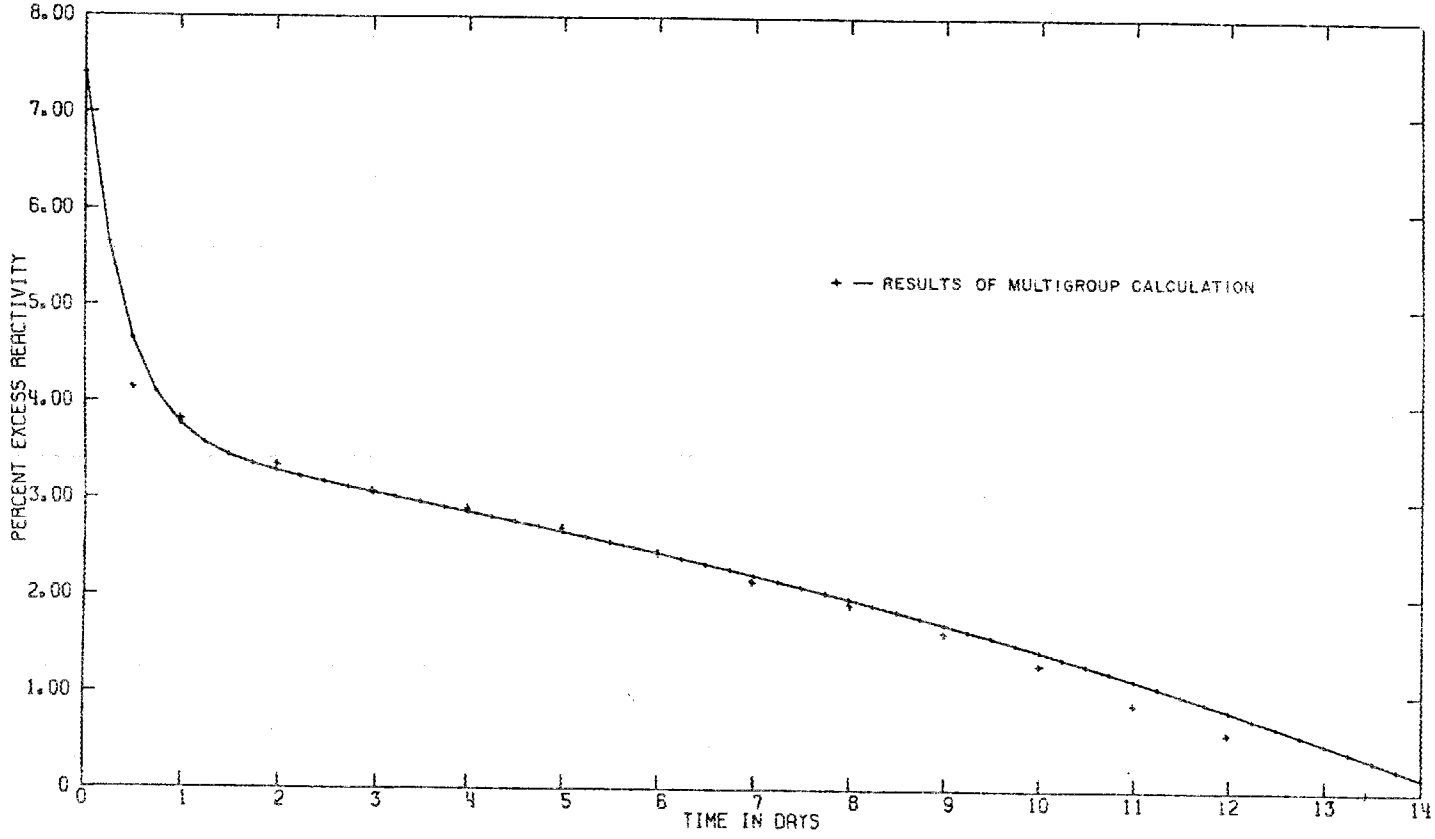

Fig. 3. HFIR Reactivity vs. Operating Time.

NOTATION

D	Diffusion coefficient
T	Temperature
$\underline{x}$	Position vector
ϕ	Neutron flux
Σ	Macroscopic cross section
k	Multiplication constant
ν	Neutrons per fission
σ	Microscopic cross section
N	Nuclide density
J	Neutron destruction operator
K	Neutron production operator
ρ	Reactivity, defined by $(k-1)/k$
ϕ^+	Adjoint neutron flux, neutron importance
V	Volume
T_r	Average temperature of region r
$\phi^{(r)}$	Average neutron flux in region r
$N_i^{(r)}$	Average concentration of nuclide i in region r
$\sigma_i^{(r)}$	Effective microscopic cross section for nuclide i in region r, as defined by Eq. 6
$\Sigma^{(r)}$	Effective macroscopic cross section in region r
$\alpha^{(r)}$	Temperature coefficient of reactivity of region r
$\tilde{\sigma}_i^{(r)}$	Effective microscopic cross section for nuclide i in region r, as defined by Eq. 18
s	Effective shim plate position
α, β	Constants determined from reactor physics calculations
M_f	Mass of fuel

C_f	Specific heat of fuel
Γ_f	Fraction of the total heat source that appears in the fuel
Γ	Heat energy produced per fission
h_{fc}	Heat transfer coefficient for heat transfer from fuel to fuel coolant
A_f	Heat transfer area for heat transfer from fuel to fuel coolant
M_c	Mass of fuel coolant in the core at any time
C_c	Specific heat at constant volume for fuel coolant
τ_c	Core transit time for fuel coolant
T_{in}	Temperature of fuel coolant at inlet to core, assumed fixed
γ_h	Fraction of thermal power delayed
w	Delayed thermal power
Ψ	Total heat source

Subscripts

a	Absorption
c	Capture
f	Fission
n2n	Be(n,2n) reaction
nα	Be(n,α) reaction
i	Nuclide i
r	Region r
5	^{235}U
10	^{10}B
I	^{135}I
xe	^{135}Xe
pm	Pseudo Pm isotope
sm	^{149}Sm

FP	Fission products other than ^{135}Xe and ^{149}Sm
Li	^{6}Li
in	Reactor inlet

Superscripts

(r)	Region r
(s)	Region s

APPENDIX I

FORTRAN PROGRAM SC

```
      PROGRAM SC
      DIMENSION R(8),BI(8),DO(8),DI(8)
      COMMON F3,F7,SA5S3,SA10S3,SF5S3,USF53,RNA
      COMMON SAIS3,SAXES3,SAPMS3,SASMS3,SALIS7
      COMMON AMDAI,AMDAXE,AMDAPM,GI,GXE,GPM,GSM,ALPFP,V3,V7
      READ 1,SA5S3,SA53,USF53,SF5S3
      PRINT1,SA5S3,SA53,USF53,SF5S3
      READ 1,SA10S3,SA103
      PRINT1,SA10S3,SA103
      READ 1,SAIS3,AMDAI,GI
      PRINT1,SAIS3,AMDAI,GI
      READ 1,SAXES3,SAXE3,AMDAXE,GXE
      PRINT1,SAXES3,SAXE3,AMDAXE,GXE
      READ 1,SAPMS3,AMDAPM,GPM
      PRINT1,SAPMS3,AMDAPM,GPM
      READ 1,SASMS3,SASM3,GSM
      PRINT1,SASMS3,SASM3,GSM
      READ 1,ALPFP
      PRINT1,ALPFP
      READ 1,SALIS7,SALI7,RN2N,RNA
      PRINT1,SALIS7,SALI7,RN2N,RNA
      READ 1,V3,V7
      PRINT1,V3,V7
      READ 1,BETA7,GAM7
      PRINT1,BETA7,GAM7
      READ 1,TFIN,DT,ANI,ANP
      PRINT1,TFIN,DT,ANI,ANP
      READ 1,B
    1 FORMAT(7E11.3)
    2 FORMAT(8E11.3)
      DO 88 NI = 1,51,10
      ANI = NI
      NP=ANP
      DRFCSM=0.0
      DR5SM=0.0
      DR10SM=0.0
      DRXESM=0.0
      DRSMSM=0.0
      DRFPSM=0.0
      DRLISM=0.0
      T=0.0
      TDAYS=0.0
      NC=0
      H=DT/ANI
      PRINT 1,TDAYS
      PRINT 1,DR5SM,DR10SM,DRXESM,DRSMSM,DRFPSM,DRLISM,DRHOSM
      PRINT2,B
```

```
    6 CALL INTERP(T,F3,S,AK)
      F7=(BETA7*S+GAM7)*F3
      CONST3=(F3**2)*V3
      CONST7=(F7**2)*V7
      DO 14 J=1,NI
      IF(J-1)19,21,19
   19 CALL INTERP(T,F3,S,AK)
   21 CALL EQUA(T,B,DO)
      IF(J-1)17,18,17
   18 DEN=USF53*B(1)*CONST3*(1.0+RN2N*(GAM7+BETA7*S))
      CONST=DT/DEN
      DR5=(USF53*DO(1)/AK-SA53*DO(1))*CONST3*CONST
      DR10=-SA103*DO(2)*CONST3*CONST
      DRXE=-SAXE3*DO(4)*CONST3*CONST
      DRSM=-SASM3*DO(6)*CONST3*CONST
      DRFP=-DO(7)*CONST3*CONST
      DRLI=-SALI7*DO(8)*CONST7*CONST
      DR=DR5+DR10+DRXE+DRSM+DRFP+DRLI
      DRHOSM=DRHOSM+DR
      DR5SM=DR5SM+DR5
      DR10SM=DR10SM+DR10
      DRXESM=DRXESM+DRXE
      DRSMSM=DRSMSM+DRSM
      DRFPSM=DRFPSM+DRFP
      DRLISM=DRLISM+DRLI
   17 T=T+H
      DO 13 I=1,8
   13 B1(I)=B(I)+H*DO(I)
      CALL EQUA(T,B1,D1)
      DO 14 I=1,8
   14 B(I)=B(I)+H*(DO(I)+D1(I))*0.5
      NC=NC+1
      IF(NC-NP)12,11,11
   11 TDAYS=T/8.64E+4
      PRINT 1,TDAYS
      PRINT 1,DR5SM,DR10SM,DRXESM,DRSMSM,DRFPSM,DRLISM,DRHOSM
      PRINT 2,B
      NC=0
   12 IF(T-TFIN)6,8,8
    8 B(1) = 4.726E+20
      B(2) = 3.303E+18
      B(3)=B(4)=B(5)=B(6)=B(7)=B(8)=0.0
   88 CONTINUE
    9 END SC
```

```
      SUBROUTINE EQUA(T,B,D)
      DIMENSION B(8),D(8)
      COMMON F3,F7,SA5S3,SA10S3,SF5S3,USF53,RNA
      COMMON SAIS3,SAXES3,SAPMS3,SASMS3,SALIS7
      COMMON AMDAI,AMDAXE,AMDAPM,GI,GXE,GPM,GSM,ALPFP,V3,V7
      D(1)=-F3*SA5S3*B(1)
      D(2)=-F3*SA10S3*B(2)
      D(3)=GI*F3*SF5S3*B(1)-(AMDAI+F3*SAIS3)*B(3)
      D(4)=GXE*F3*SF5S3*B(1)+AMDAI*B(3)-(AMDAXE+F3*SAXES3)*B(4)
      D(5)=GPM*F3*SF5S3*B(1)-(AMDAPM+F3*SAPMS3)*B(5)
      D(6)=GSM*F3*SF5S3*B(1)+AMDAPM*B(5)-SASMS3*F3*B(6)
      D(7)=ALPFP*F3*SF5S3*B(1)
      D(8)=RNA*USF53*B(1)*F3*V3/V7-SALIS7*F7*B(8)
      RETURN
      END
```

```
      SUBROUTINE INTERP(T,X3,S,AK)
      COMMON F3,F7,SA5S3
      S=0.0
      AK=1.0
      X3=3.329E+14/(1.0-SA5S3*(3.329E+14)*T)
      RETURN
      END
```

INTERNAL DISTRIBUTION

1. R.K. Adams
2. J.L. Anderson
3. S.J. Ball
4. A.E.G. Bates
5. F.T. Binford
6. A.L. Boch
7. C.J. Borkowski
8-27. J.B. Bullock
28. O.W. Burke
29. R.D. Cheverton
30. T.E. Cole
31. J.A. Cox
32. F.L. Culler
33. R.A. Dandl
34. H.P. Danforth
35. S.J. Ditto
36. E.P. Epler
37. D.N. Fry
38. C.S. Harrill
39. W.H. Jordan
40. T.W. Kerlin
41. R.C. Kryter
42. C.D. Martin
43. L.C. Oakes
44. H.G. O'Brien
45. G.R. Owens
46. D.P. Roux
47. P. Rubel
48. G.S. Sadowski
49. T.M. Sims
50. R.S. Stone
51. C.S. Walker
52. K.W. West
53. J.W. Woody
54-55. Central Research Library
56. Document Reference Section
57-59. Laboratory Records Department
60. Laboratory Records, ORNL R.C.
61. ORNL Patent Office
62-76. Division of Technical Information Extension
77. Research and Development Division, ORO

EXTERNAL DISTRIBUTION

78. S.H. Hanauer, Univ. Tenn.
79. J.C. Robinson, Univ. Tenn.
80. J.R. Trinko, Univ. Tenn.
81-86. B.R. Lawrence, Australian AEC
87. F.C. Legler, AEC, Washington, D.C.